Improvement of the Performance of a Centrifugal Compressor by Modifying the Volute Inlet

Semi Kim
Department of Mechanical Engineering,
POSTECH,
San 31, Hyoja-dong, Nam-gu,
Pohang 790-784, Korea
e-mail: ssemlove@postech.ac.kr

Junyoung Park
Senior Researcher
e-mail: jypark@kimm.re.kr

Kukyoung Ahn
President Researcher
e-mail: kyahn@kimm.re.kr

KIMM,
Sinseongno, Yuseong-gu,
Daejeon 305-343, Korea

Jehyun Baek[1]
Professor
Department of Mechanical Engineering,
POSTECH,
San 31, Hyoja-dong, Nam-gu,
Pohang 790-784, Korea
e-mail: jhbaek@postech.ac.kr

In centrifugal compressors, the diffuser and the volute have strong influences on the flow discharged from the impeller and thus also on the performance. In particular, a key parameter is the radial velocity at the volute inlet; it determines the swirl velocity, which is dissipated as a loss, i.e., it results in performance degradation. With the aim of reducing the swirl loss, a new type of volute with a modified inlet height was tested in this study. The volute inlet height was modified to 6 mm and 7 mm from the original height of 5 mm. The reliability of our computations was tested by comparison of the results of a model with this original height with experimental data. Flow analyses were conducted not only at the design mass flow rate but also at lower and higher mass flow rates. A higher total-to-total efficiency was obtained as a result of the linear increases of the volute inlet height from the diffuser outlet to 6 mm and 7 mm. Our detailed investigation of the simulated flow fields shows that the flow characteristics for a volute inlet height of 6 mm are better than those for a volute inlet height of 5 mm. These results clearly show that a greater volute inlet height assists in pressure recovery and reduces swirl loss in the volute. However, the volute inlet height of 7 mm results in larger hub separation and more energy loss, and thus in inferior performance. Therefore, the hub separation and the radial velocity at the volute inlet strongly influence the performance.
[DOI: 10.1115/1.4001972]

Keywords: centrifugal compressor, volute inlet height, total-to-total efficiency, off-design analysis

1 Introduction

In centrifugal compressor systems, the diffuser and volute have strong influences on the flow passing through the impeller and thus also on performance. Diffusers are either vaneless or vaned and recover static pressure from the high kinetic energy of the impeller. The volute is a passage located circumferentially around the diffuser exit that collects the flow from the diffuser and delivers it to the exit flange. The cross-sectional area of the volute passage increases in circumference, so another function of the volute is the recovery of static pressure from the remaining momentum energy. To enable effective pressure recovery, the flow passage needs to be sufficiently long. However, the design of the diffuser and volute is commonly constrained by restrictions, such as the maximum casing size and the location of the exit pipe. As a compromise between compact size and performance, an intermediate volute with a mean cross-sectional radius that is the same as the radius of the volute inlet is used in this study.

Volute flow has often been studied with the aim of improving compressor performance, with particular focus on the interaction between the impeller and the diffuser, the main flow phenomena, and the loss mechanisms [1–6]. In previous analyses of volutes, consideration of the loss mechanisms has been an effective means of improving volute performance [1,2,4–6]. It is obvious that the volute cannot recover the radial (meridional) velocity head at the diffuser exit and that a component of the flow velocity becomes a swirl component in the volute, which will eventually be dissipated. Since the swirl velocity component in the volute is a main cause of performance degradation, the reduction of swirl loss might result in improvements in the performance of the system.

To achieve such improvements for a fixed casing size, some additional space is necessary to decelerate the radial component of the flow velocity and to completely recover this velocity head to static pressure. In this study, an alternative geometry with area expansion in both the radial and axial directions was investigated. Additional deceleration is obtained by linearly increasing the height from the diffuser vane exit to the volute inlet; the swirl velocity is then expected to decrease, which should mean that the loss due to secondary flow in the volute is diminished and that the circumferential pressure recovery is improved. This new design is expected to be one alternative between smaller size of whole system and better performance.

Furthermore, since off-design operation strongly influences centrifugal compressor flow, flow analyses at low and high mass flow rates were also conducted. In total, three types of centrifugal compressors, one with the original volute and the other two with modified volute inlets, were investigated. In order to test the validity of these numerical calculations, experimental results were compared with the computational fluid dynamics (CFD) results.

2 Compressor Stage Description

The compressor stage consists of a centrifugal impeller with 15 blades and a vaned diffuser with 17 vanes. The impeller is unshrouded with a constant tip clearance of 0.3 mm. The diffuser vanes have a constant height equal to the impeller exit height, 5 mm. The main geometrical configuration and parameters are listed in Fig. 1 and Table 1.

The cross-sectional area of the volute increases circumferentially according to the principles of conservation of mass and angular momentum. The flow in the volute is not uniform over the cross-sectional area: distorted profiles, viscosity effects, and secondary flows tend to produce an actual mean velocity somewhat higher than that calculated with the ideal model [7]. Thus, a sizing

[1]Corresponding author.

Contributed by the Fluids Engineering Division of ASME for publication in the JOURNAL OF FLUIDS ENGINEERING. Manuscript received October 25, 2009; final manuscript received June 9, 2010; published online September 3, 2010. Assoc. Editor: Chunill Hah.

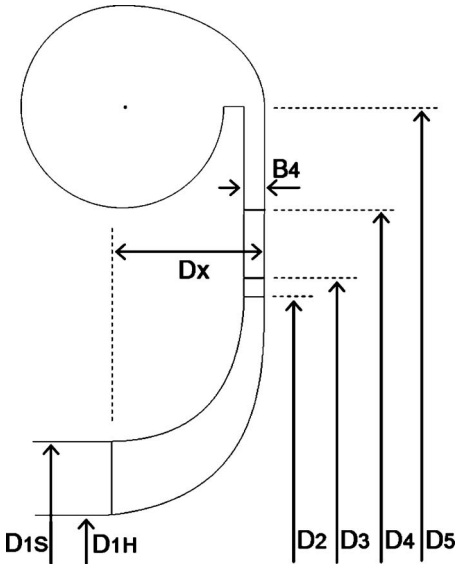

Fig. 1 Geometrical configuration and parameters of the compressor

parameter, SP, of 1.11 was used as the ratio of the actual volute area to the value satisfying the principle of ideal conservation of angular momentum.

3 Computational Procedure

The numerical model was created and analyzed by using ICEM-CFD and ANSYS CFX, respectively. The impeller and diffuser were discretized by using an H-type grid with $72\times46\times35$ and $55\times48\times18$ points, respectively, in the streamwise, pitchwise, and spanwise directions. An H-type grid with 320,000 nodes was used for the volute mesh, and a tetratype grid with 70,000 nodes was used near the tongue due to its complex geometry. Ten cells were placed for impeller tip clearance.

The k-ω SST model was used for the turbulence, and the mixing plane model, which computes circumferentially averaged profiles of flow variables, was used for interpolation at the interface of the rotating impeller and the stationary diffuser parts. The design rotational speed was 50,000 rpm and the inlet and outlet boundary conditions were the total pressure and the mass flow rate, respectively.

Table 1 Specification of the geometrical parameters

Impeller	
Blade number	15
Inlet hub diameter (D_{1H})	36.0 mm
Inlet shroud diameter (D_{1S})	71.5 mm
Inlet tip angle	47 deg (from tangential)
Exit diameter (D_2)	140.0 mm
Tip clearance	0.3 mm
Exit angle	50 deg (from tangential)
Diffuser	
Blade number	17
Inlet diameter (D_3)	148.4 mm
Inlet angle	20 deg (from tangential)
Exit diameter (D_4)	185.6 mm
Axial length (Δx)	140.0 mm
Blade height (B_4)	5.0 mm
Exit angle	29 deg (from tangential)
Volute	
Inlet diameter (D5)	228.0 mm

Table 2 Aerodynamic specifications

Required boundary conditions	Values
Inlet total pressure	100,000 Pa
Inlet total temperature	298 K
Outlet mass flow rate	0.3 kg/s
Rotational speed rpm	50,000
Specific heat ratio	1.4

The design specifications for the flow calculations are listed in Table 2. A two-dimensional view of the full system is shown in Fig. 2 and the detailed surface grid of the impeller and the cross-sectional grid of the volute are shown in Fig. 3. The tongue of the volute is located at $\theta=42.7$ deg in Fig. 2.

4 Experiments and Validation

To validate these numerical calculations, a compressor map is drawn with CFD and experimental results. The test rig consists of the impeller, diffuser, and volute, and a Kiel probe was used as the measurement device. Only the total pressures at the impeller inlet and the volute exit were measured at rotation speeds of 35,000 and 40,000 rpm because of some technical limitations. Figure 4 shows the configuration of the impeller and Fig. 5 shows a photograph of the experimental setup.

The experimental results are compared with the CFD results in Fig. 6. The CFD results are in good quantitative and qualitative agreement with the experimental results in most flow rate regions except in the high mass flow rate region. This difference arises because CFD underestimates the outlet pressure under near choking conditions, which results in a steep decline in the total pressure ratio.

We conclude that this comparison validates the numerical calculations using the ANSYS CFX solver.

5 Modified Volute Geometries

The initial volute is an overhung type volute, which is one of the intermediate volutes; its cross-sectional shape is shown in Fig. 3. The diffuser height is fixed at 5 mm from the inlet to the outlet and is the same as the volute inlet height. In order to reduce

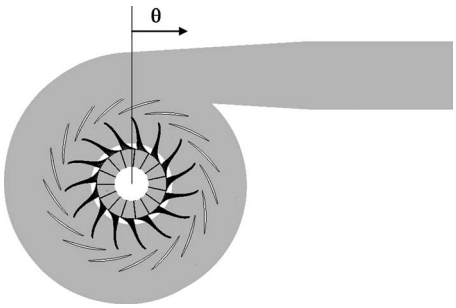

Fig. 2 Full 2D view of the compressor

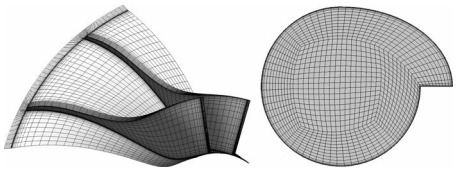

Fig. 3 Detailed surface grid of the impeller and cross-sectional grid of the volute

Fig. 4 The impeller

swirling loss in the volute and improve performance, a new volute concept is proposed in this paper. By changing the volute inlet height linearly from the diffuser exit, the radial velocity component can be transformed into static pressure more effectively. When the volute inlet heights are increased by 1 mm and 2 mm, new models with volute inlet heights of 6 mm and 7 mm, respectively, are obtained. The configurations of the three volutes are shown in Fig. 7. Volutes B and C have diffusion angles in the meridional plane of 2.7 deg and 5.4 deg, and the ratios of the volute inlet area to the diffuser exit area are 1.228, 1.474, and 1.720 for volutes A, B, and C, respectively.

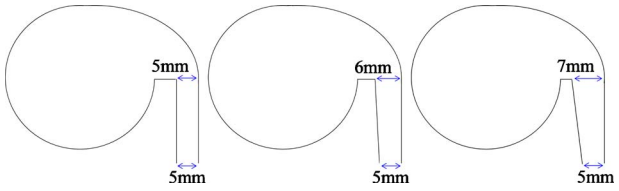

Fig. 7 Schematic diagrams of the modified volute configurations

In this study, the following centrifuge compressors with 15 impellers and 17 diffuser vanes were analyzed:

a. Case 1: volute A (inlet height 5 mm)
b. Case 2: volute B (inlet height 6 mm)
c. Case 3: volute C (inlet height 7 mm)

6 Result and Performance Improvement

Three-dimensional flow field calculations were conducted for the design mass flow rate of 0.3 kg/s and the total-to-total efficiency and total pressure ratio were obtained, as shown in Table 3. Case 2 exhibits the best performance, with an improvement in efficiency of 0.37%. The performance of Case 3 is slightly better than that of Case 1.

7 Flow Analysis

The improvements in performance shown in Table 3 can be explained with the flow analyses for the diffuser and volute discussed below.

7.1 Swirl Velocity, Cp, and ω . Figure 8 shows the calculated distributions of the velocity in vector form for four cross sections of the volute. The cross sections are at 90 deg (plane 1), 180 deg (plane 2), 270 deg (plane 3), and 360 deg (plane 4), as shown in Fig. 2.

For all cases, the swirl distribution shows that the swirl velocity

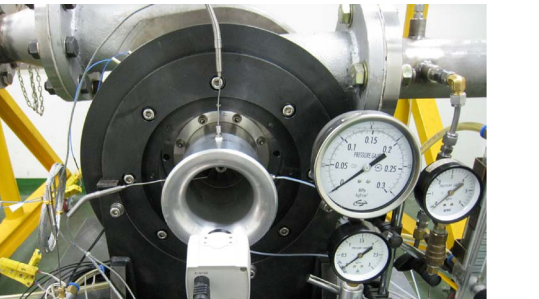

Fig. 5 The experimental setup

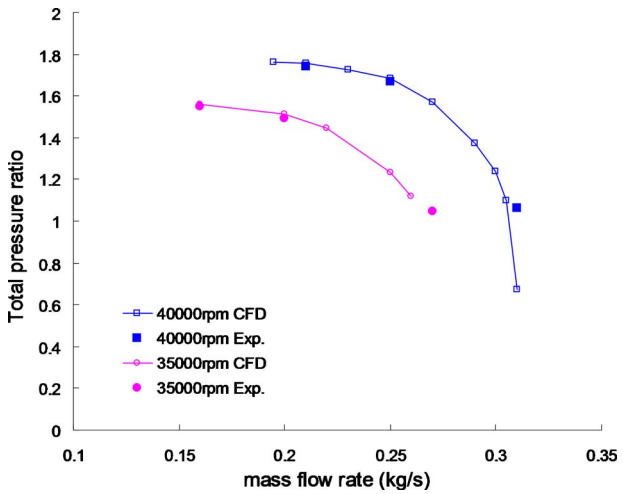

Fig. 6 Total pressure ratios for the original model at 35,000 rpm and 40,000 rpm

Table 3 The total-to-total efficiencies and total pressure ratios of cases 1–3

	Total-to-total efficiency (%)	Total pressure ratio
Case 1	81.86	2.308
Case 2	82.23	2.312
Case 3	81.97	2.310

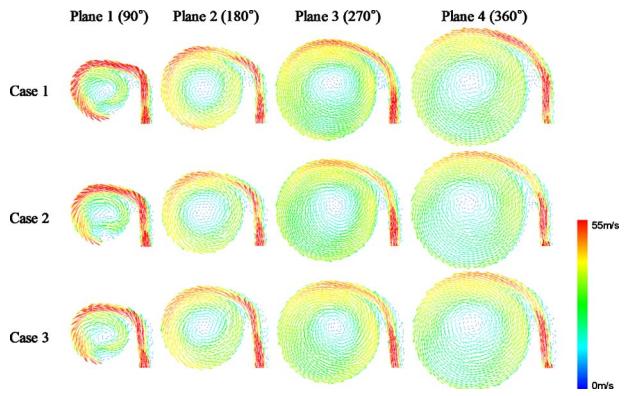

Fig. 8 Velocity distributions in four cross sections of the volute

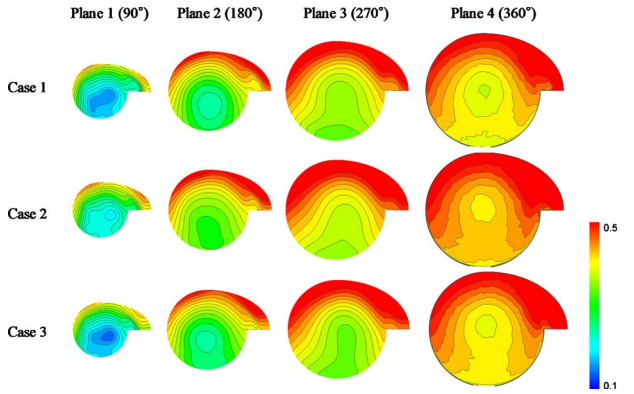

Fig. 9 Distributions of the pressure recovery coefficients for the four cross sections of the volute

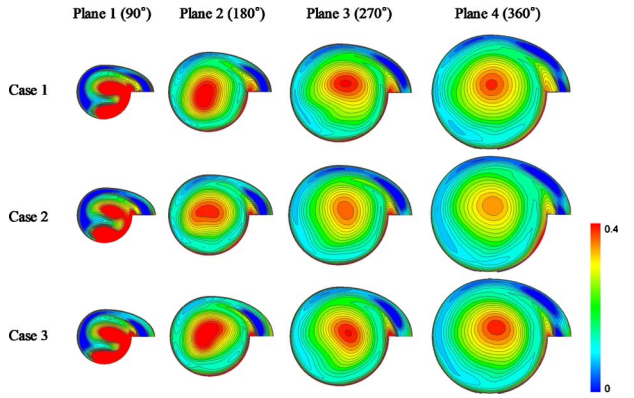

Fig. 10 Distributions of the total pressure loss coefficients for the four cross sections of the volute

is almost constant near the walls, forming a forced vortex type flow in the center. A detached flow appears on the hub side in the vicinity of the volute inlet and this hub separation extends into the volute. The hub detachment is thought to originate from a complex flow pattern generated at the interface between the moving impeller hub and the stationary diffuser wall and to finally become a blockage near the hub. This blockage pushes the flow toward the shroud, forcing the flow to pass through a small area and thus accelerate. This process results in an increase in the flow velocity near the shroud of the diffuser. Furthermore, due to the sudden expansion of the diffuser-volute interface, a circulation region is also found on the diffuser shroud side in the volute.

The radial velocity in the volute is the main source of loss and decline in the volute performance. In case 1, the higher radial velocity near the shroud turns toward the volute and rotates along the wall; the stronger swirl velocity in case 1 can be found in all 4 planes. In cases 2 and 3, the radial velocity component decreases due to the increases in the cross-sectional area between the diffuser exit and the volute inlet, i.e., as the volute inlet height increases linearly from the diffuser exit. The reduction in the radial velocity at the volute inlet is directly connected to the decrease in the swirl velocity and swirl loss in the volute.

The distributions of the pressure recovery coefficient Cp:

$$C_P = \frac{P - \bar{P}_4}{\bar{P}_4^0 - \bar{P}_4} \tag{1}$$

are shown for four cross sections of the volute in Fig. 9. Cp is the ratio of the static pressure rise to the dynamic pressure at the diffuser outlet. Therefore, a high Cp means that effective pressure recovery occurs between the diffuser outlet and the volute. The conservation of angular momentum and the centrifugal forces resulting from the circumferential velocity should lead to a radially increasing pressure; in fact, a remarkable pressure difference between the volute center and the walls arises, as is shown in Fig. 8(*b*). Furthermore, the Cp contours at 360 deg (plane 4) are not smooth compared with those for planes 1, 2, and 3, and exhibit a saw-toothed pattern. Since the whole flow is collected from a circumferential passage near the tongue, it is usually quite unstable with a complex flow pattern.

The comparison of planes 1 to 4 for case 2 shows that the circumferential velocity is effectively transformed into static pressure in the volute. Compared with the results for the original volute, i.e., case 1, case 3 has somewhat higher Cp in planes 2 and 4 and lower Cp in planes 1 and 3, but the results are similar.

A high swirl velocity at the volute wall and a high velocity gradient at the vortex center are both important sources of loss. Figure 10 shows the distribution of the total pressure loss coefficient ω:

$$\varpi = \frac{\bar{P}_4^0 - P^0}{\bar{P}_4^0 - \bar{P}_4} \tag{2}$$

ω is the ratio of the total pressure loss to the dynamic pressure at the diffuser outlet and is a dimensionless parameter. At vortex center, there exits a vortex type flow and high ω is obtained. The deficit in the total pressure at the center of the vortex is due to the high shear. A low total pressure and high throughflow velocity at the center result in a low core static pressure, as shown in Fig. 9. However, there is no rigid body vortex in plane 1 because the highest ω arises not only at the center but also at the radially inner wall.

The distribution with the lowest ω values arises in case 2; cases 1 and 3 exhibit similar distributions of ω. This result is in accord with the observation that the performance and flow pattern in case 2 are improved by the modification of the volute inlet height.

7.2 Radial and Circumferential Velocities at the Volute Inlet. In Fig. 8, a higher radial velocity was found near the shroud because of hub separation, so the main flow is concentrated with a slant toward the shroud before entering the volute. As mentioned above, the radial velocity component behind the diffuser vanes is eventually dissipated as a swirl loss in the volute passage. It is obvious that the best volute is one with a relatively small swirl velocity; the radial velocities at the volute inlet from hub to shroud for cases 1, 2, and 3 are compared in Fig. 11.

The radial velocity of case 3 is the lowest over almost the whole range, except near the shroud, and the largest value arises in case 1. In the spanwise direction, the averaged-radial velocities

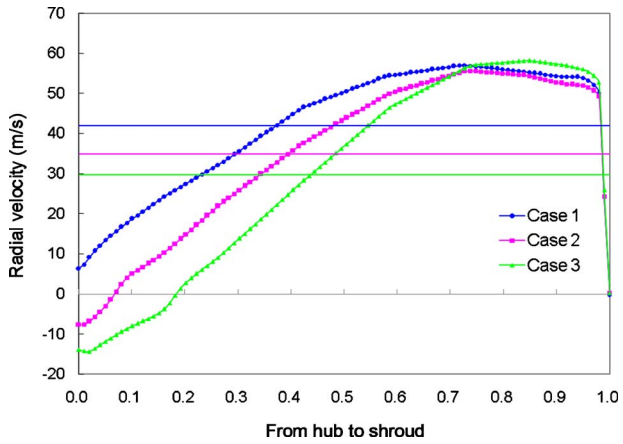

Fig. 11 Radial velocity distributions from hub to shroud at the volute inlet

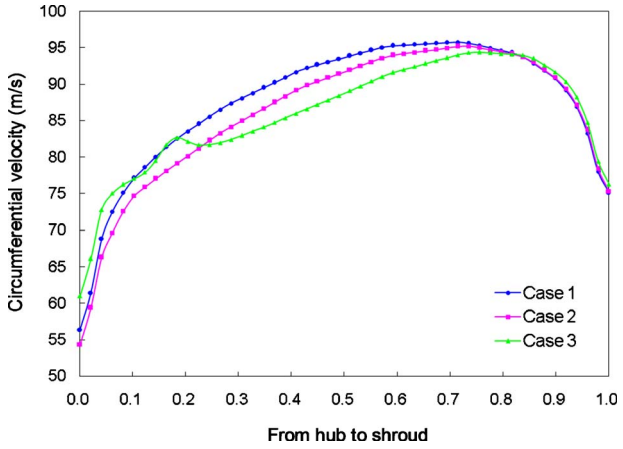

Fig. 12 Circumferential velocity distributions from hub to shroud at the volute inlet

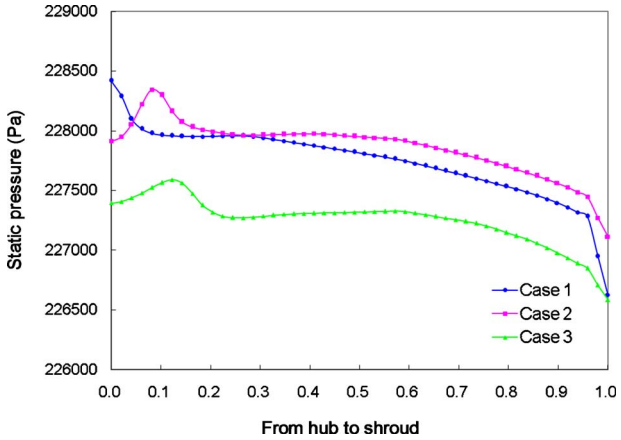

Fig. 13 Static pressure distributions from hub to shroud at the volute inlet

are 41.9 m/s, 34.9 m/s, and 29.7 m/s for cases 1, 2, and 3, respectively. Since the height of the volute inlet is largest in case 3 and the radial velocity in case 3 is reduced by conservation of mass, the radial velocity of case 3 is expected to be lower than that of case 1. However, although case 3 has a volute inlet height of 7 mm, the radial velocity of case 3 near the shroud is higher than those found for the models with volute inlet heights of 5 mm and 6 mm. In other words, when the volute inlet is too wide, as in case 3, the hub separation becomes larger, as shown in Fig. 8, and the flow is pushed toward the shroud. As a result, the radial velocity near the shroud in case 3 is higher than in the other cases. Furthermore, due to the hub separation, a negative radial velocity arises near the hub for cases 2 and 3, but a much larger negative region arises for case 3.

Figure 12 shows the distribution of the circumferential velocity from hub to shroud at the volute inlet. Since the circumferential velocity is converted into static pressure through the volute passage, higher circumferential velocity at the volute inlet could guarantee the higher pressure ratio at the volute outlet. In the almost spanwise region, case 1 has the highest circumferential velocity and case 3 has the lowest. These results can be analyzed in the same manner as described for Fig. 11. However, in case 3 the circumferential velocity near the hub is also high, which arises because of the unstable flow patterns due to the large hub separation.

7.3 Static Pressure Recovery. In Figs. 11 and 12, the radial and circumferential velocities decrease as the volute inlet height increases. It is important to ascertain whether the low velocity at the volute inlet is due to sufficient static pressure recovery or severe loss. With this aim in mind, the static pressure distributions from hub to shroud at the volute inlet and the static pressure distributions from the diffuser outlet to the volute inlet at midspan were plotted in Figs. 13 and 14, respectively.

In Figs. 13 and 14, it can be seen that the highest static pressure from the diffuser outlet to the volute inlet arises in case 2. The increase in the volute inlet height to 6 mm is thus effective in the recovery of the static pressure; the reason for the low velocity at the volute inlet is the efficient pressure recovery due to the appropriate area expansion.

Note that in Fig. 13 the pressure in case 3 is slightly lower than that in case 1. Beyond the diffuser vanes, the height increases linearly and the cross-sectional area undergoes a quadratic increase. Case 3 has a volute inlet height that is 1.4 times that of case 1 and the cross-sectional area at the volute inlet is 1.72 times as large as that of case 1. In case 3, the sudden expansion of the cross-sectional area results in a large hub separation and a large energy loss from the flow into the volute arises. These effects result in a low circumferential velocity (Fig. 12) and a low static pressure (Fig. 14) at the volute inlet. However, as shown in Table 3, the performance of case 3 is better than that of case 1. The reason for this difference is that the large energy loss generated by the large hub separation is compensated for by the low swirl loss due to the low radial velocity component in the volute.

7.4 Circumferential Flow Angles. The variation in the flow angles at the volute inlet between the cases is further illustrated in Fig. 15. The flow angles from the tangential direction at spans 0.1, 0.5, and 0.9 are shown for the three cases. When the flow angle is small, the flow tends to be more circumferential and the portion of kinetic energy that is transformed into swirl loss becomes relatively small.

For all spans, the flow angles fluctuate with respect to the circumferential angle and the distributions contain 17 peaks because of disturbances due to the diffuser vanes. It can be seen that the wake due to the diffuser vanes persists up to the volute inlet. Note that the flow angle is lower in case 2 than in case 1. Thus the flow in case 2 enters the volute more tangentially and less radially, which is consistent with the results in Fig. 9.

On the other hand, note that the flow in case 3 is more tangential than in case 2, as shown in Fig. 15. However, a higher total pressure ratio and a higher efficiency are obtained in case 2, as shown in Table 3. Case 3 not only has a low flow angle but also has a low circumferential velocity and a low static pressure because of the large hub separation. These flow characteristics result in degradation of the performance and in more loss than in the

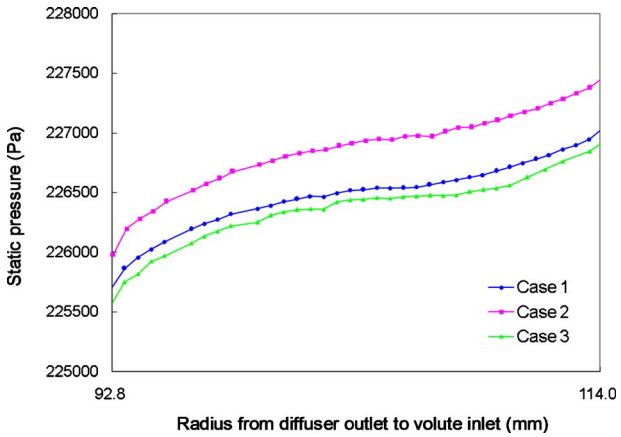

Fig. 14 Static pressure distributions from the diffuser outlet to the volute

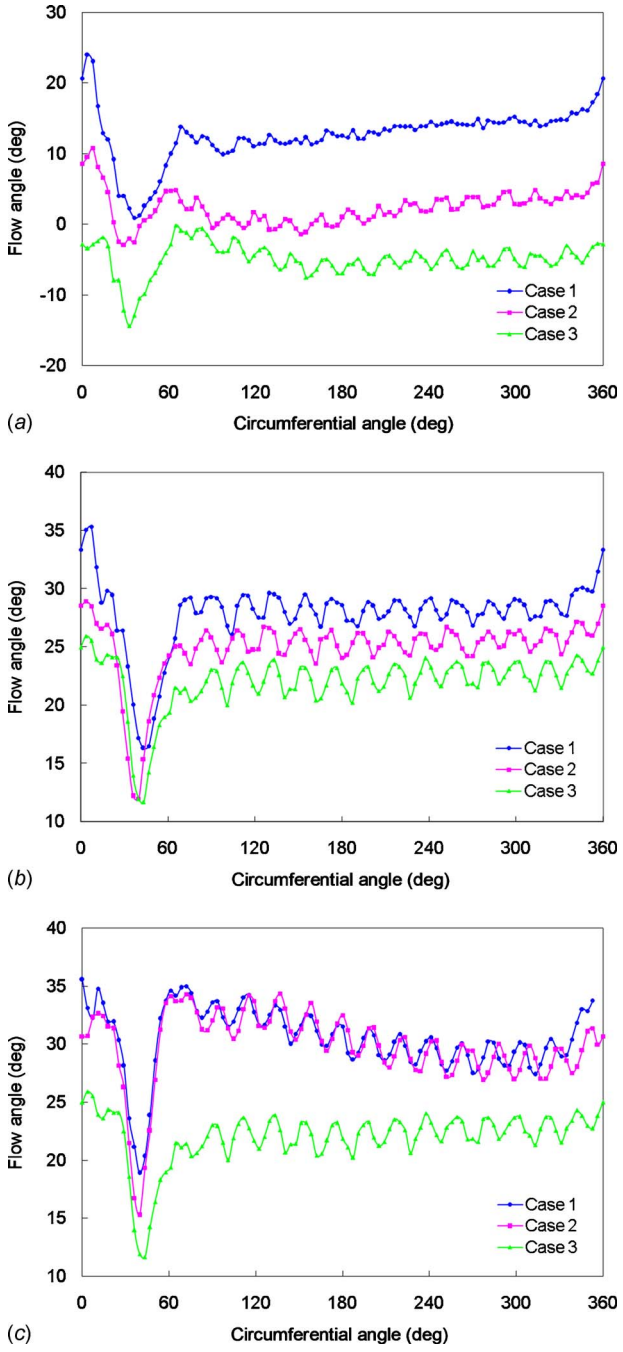

Fig. 15 Circumferential distributions of the flow angle for various span locations: (*a*) near hub (0.1 span), (*b*) at midspan (0.5 span), and (*c*) near shroud (0.9 span)

other cases.

In Fig. 15(*a*) (span 0.1, hub), it can be seen that the flow angle is highest in case 1 and that case 3 has the lowest circumferential flow angle. Negative flow angles arise near 30 deg for case 2 and for almost all the circumferential angles in case 3. A negative flow angle indicates that there is back flow at the volute inlet. In case 2, there is a small region where back flow appears near the hub, which has an insignificant effect on the performance. In case 3, back flow occurs throughout the whole circumferential area at the hub, resulting in significant loss and negative effects on the flow characteristics and performance.

In Figs. 15(*a*)–15(*c*), it can be seen that steep decreases in the flow angle arise near 40 deg, in the vicinity of the tongue. In this region, just before passing through the tongue, most of the mass flow is collected and a relatively higher static pressure is developed, as shown in Fig. 9. Under the influence of the main stream near the tongue, the radial velocity component is disturbed and the flow becomes tangential. Moreover, the fluctuation of the flow angle in the hub region is weaker than that in the midspan or shroud regions. Near the hub, there is a low velocity region owing to flow separation that reduces the effects of the diffuser vanes on the flow.

Table 4 The total-to-total efficiencies at low and high mass flow rates

	Low mass flow rate (0.27 kg/s) (%)	High mass flow rate (0.36 kg/s) (%)
Case 1	80.44	75.56
Case 2	80.62	76.30
Case 3	80.57	76.19

8 Off-Design Analysis

The above analysis was carried out at a design mass flow rate of $\dot{m}_d$=0.3 kg/s. In order to analyze the performance under off-design conditions, numerical calculations at low (0.27 kg/s, 90% of $\dot{m}_d$) and high (0.36 kg/s, 120% of $\dot{m}_d$) mass flow rates were also performed.

In Table 4, the efficiencies of cases 2 and 3 are higher at both low and high mass flow rates; case 2 has the highest efficiency, as for the design mass flow rate.

The improvement ratio is larger for the high mass flow rate than for the low mass flow rate. At the high mass flow rate, the hub separation becomes small and the flow is distributed relatively uniformly in the spanwise direction due to the high momentum energy. Furthermore, in cases 2 and 3, the radial velocity of the high speed flow decreases because of the axial and radial area expansions, and this might be the reason for the performance improvement.

At the low mass flow rate, although the radial velocity and swirl loss are reduced, a larger hub separation results from the low momentum energy, so the improvement is thus smaller than at the high mass flow rate because of the opposing effects of low swirl loss and large hub separation.

9 Conclusion

A study of the improvements in performance of a centrifugal compressor resulting from linear increases in the volute inlet height from the diffuser outlet has been performed. The influence of the volute inlet height on the efficiency and pressure ratio was investigated, and detailed flow simulations were carried out, in order to determine the reason for the improved performance.

1. The radial velocity at the volute inlet becomes weaker due to the increased volute inlet height. Accordingly, the induced swirl velocity, which is rotating along the volute wall decreases in cases 2 and 3. The loss due to swirl can be effectively reduced by increasing the volute inlet height, which results in improved performance.
2. Hub separation is generated by unstable interactions between the rotating impeller and the stationary diffuser hub, and so is another key mechanism determining volute performance. A volute inlet height that is too large results in a large hub separation. Although swirl loss is decreased by the increased volute inlet height, the performance is inferior to that obtained with a medium volute inlet height because of large hub separation and low static pressure recovery. Although the hub separation increases slightly for an appropriate volute inlet height, the radial velocity is effectively converted into static pressure and the performance is improved.

3. The performance of a centrifugal compressor with a diffusing volute inlet is improved at low and high mass flow rates. At low mass flow rates, the performance improvement due to the reduction in swirl loss is small due to the comparatively large hub separation. At high mass flow rates, the decreases in the hub separation and the radial velocity result in a significant performance improvement.

Acknowledgment

This study was supported by the Korea Institute of Machinery and Materials (KIMM) and BK21.

Nomenclature

P = static pressure
P_0 = mass-averaged total pressure
T = static temperature
T_0 = mass-averaged total temperature
γ = gas specific heat ratio
η = isentropic total-to-total efficiency

Subscripts

1 = impeller inlet
2 = impeller outlet
3 = diffuser inlet
4 = diffuser outlet
5 = volute inlet
H = hub
S = shroud

References

[1] Hagelstein, D., Hillewaert, K., Braembussche, R. A., Engeda, A., Keiper, R., and Rautenberg, M., 2000, "Experimental and Numerical Investigation of the Flow in a Centrifugal Compressor Volute," ASME J. Turbomach., **122**(1), pp. 22–31.
[2] Gu, F., Engeda, A., Cave, M., and Liberti, J., 2001, "A Numerical Investigation on the Volute/Diffuser Interaction Due to the Axial Distortion at the Impeller Exit," ASME J. Fluids Eng., **123**(3), pp. 475–483.
[3] Meakhail, T., and Park, S., 2005, "A Study of Impeller-Diffuser-Volute Interaction in a Centrifugal Fan," ASME J. Turbomach., **127**(1), pp. 84–90.
[4] Braembussche. R. A., 2006, "Flow and Loss Mechanisms in Volutes of Centrifugal Pumps," RTO-EN-AVT-143.
[5] Steglich, T., Kitzinger, J., Seume, R., Braembussche, R.A., and Prinsier, J., 2008, "Improved Diffuser/Volute Combinations for Centrifugal Compressor," ASME J. Turbomach., **130**(1), p. 011014.
[6] Chen, H., Guo, S., Zhu, X., Du, Z., and Zhao, S., "Numerical Simulations of Onset of Volute Stall Inside a Centrifugal Compressor," ASME Paper No. GT2008-50036.
[7] Aungier, R., 2000, *Centrifugal Compressors*, ASME, New York.